PCCP

Accepted Manuscript

ROYAL SOCIETY OF CHEMISTRY

www.rsc.org/pccp

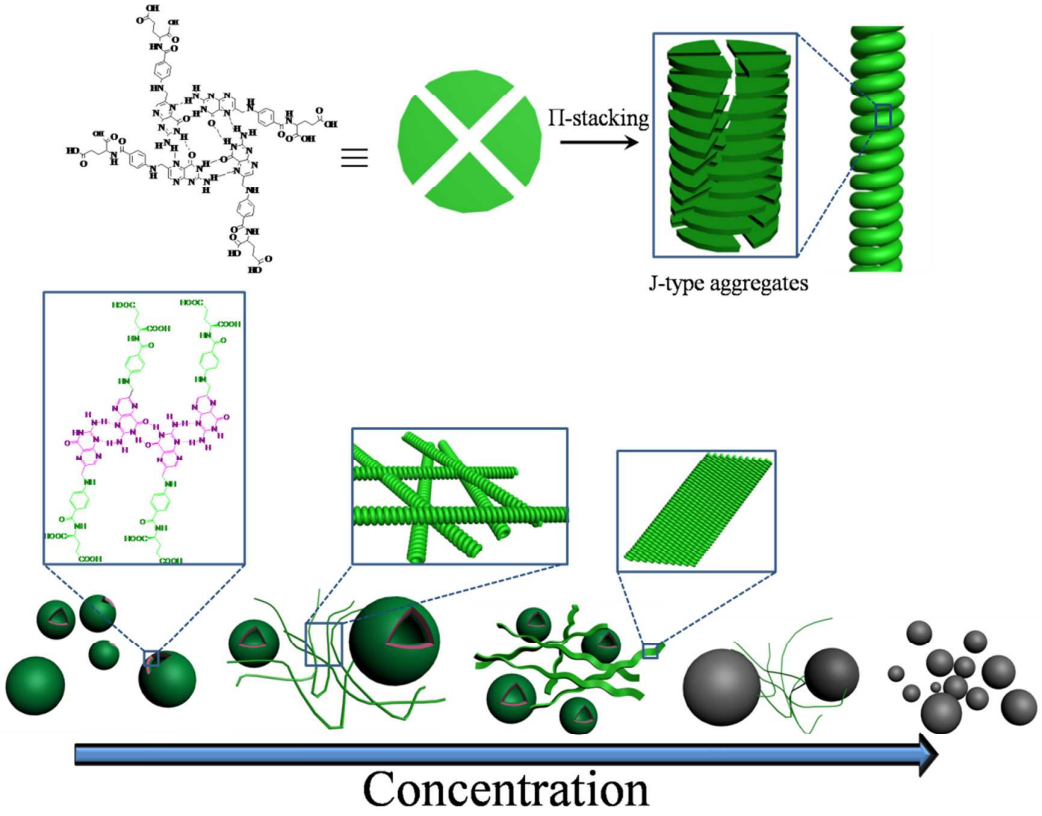

Supramolecular gel with multi-responsiveness, self-healing properties and concentration dependent orthogonal self-assemblies are constructed from folic acid via a solvent strategy.

Cite this: DOI: 10.1039/c0xx00000x

www.rsc.org/xxxxxx

ARTICLE TYPE

Supramolecular gel from folic acid with multiple responsiveness, rapid self-recovery and orthogonal self-assemblies

Pengyao Xing,[a] Xiaoxiao Chu [a] Mingfang Ma,[a] Shangyang Li,[a] and Aiyou Hao*[a]

Received (in XXX, XXX) Xth XXXXXXXXX 20XX, Accepted Xth XXXXXXXXX 20XX

DOI: 10.1039/b000000x

Through a good/poor solvent strategy, native folic acid (FA) which behaves as a super-gelator in DMSO/water system can be successfully employed to construct supramolecular gels. The system exhibited a morphological evolution with the increase of FA concentration; various phases such as vesicles, fiber/vesicles, fiber/nanoparticles, nanoparticles were probed. In the self-assembly process, L-glutamic acid moiety induced the formation of helical 1-dimensional (1-D) fibers which further self-assembled into a gel. Stimuli like heat, stress, pH and light which affect the molecular structure of FA or solubility in the mixed solvents had the pronounced influence on the properties of gels, such as mechanical properties or bulk phases. Time-dependent oscillatory stress scan indicated that the supramolecular gel had a self-healing property. Without tedious modification routes and the addition of alkali metal ions, native FA which served as an efficient building block and super-gelator to build up multi-responsive and self-recovery material was investigated for the first time.

Introduction

Materials prepared by low molecular weight molecules through non-covalent bonds have always tried to find their applications, to name a few, micelle/vesicles for drug delivery[1], liquid crystals for optical device[2], gels for cell culture[3]. Supramolecular nanoarchitectures which are constructed by reversible and directional noncovalent interactions between monomers and exhibit various functions, are a kind of remarkable material and has attracted more and more attentions beyond supramolecular chemistry.[4] For instance, supramolecular polymers have undergone processes from leading to function,[5, 6] from lab to market[7]. Over the past 20 years, monomers/building blocks have been held together through various weak interactions including H-bonds, π-π stacking, host-guest interaction and metal-ligand coordination to build up nanoarchitectures with different topologies and dimensions, such as 0D vesicles/micelles, 1D nanofibers, 2D membranes and 3D networks or gels. In that process, orthogonal interactions are often applied to obtain supramolecular structures.[8, 9] Apart from that, some remarkable characteristics such as structural self-healing[10] or shape-memory[11] are also the selling points of supramolecular self-assembled systems. To some extent, the self-healing (or recovery) can be regarded as an inherent resistance to the stimulus of applied stress (strain). However, due to the dynamic nature of self-assembled supramolecular architectures, other chemical or physical stimuli may have profound impacts on their structural change as well, which may eventually bring about bulk changes.[12] The stimuli-responsiveness has extensively expanded the functions of supramolecular architectures, from pH tailored expansion/contraction,[13] ion triggered release[14] to light controlled healing/phase transition[15].

Self-assembled 1D nanofibers may elongate and entangle into 3D networks or free-standing gels in solvents. This process involves the transition from linear fibers into entangled networks which are more applicable than the 1-D or 2-D aggregates ascribed to their macroscopic characteristics.[16] Fascinating properties of self-assembled systems such as stimuli-responsiveness, shape-memory, self-healing and their commercial uses, require the macroscopic scaled 3-D characteristics rather than viscous solutions.[17] Supramolecular gels, as the common macroscopic phase of supramolecular architectures, have applications in medical implants, electrolytes, cell culture matrixes, template and crystal growth media.[18] Apart from these applications, gels can be promising matrixes for orthogonal self-assemblies as well, where multiple aggregates or other components are embedded.[19] Types like gels/gels[20], gels/vesicles[21], gels/liquid crystals[22], gels/micelles[23], gels/inorganic particles[24], etc. have been constructed to meet some specific functions or applications. However, to achieve multiple orthogonal self-assemblies in sole system seems rather difficult and has never been reported. According to their solvent environment, supramolecular gels are classified into two categories: organogel and hydrogel.[18] Nevertheless, a special organo-hydrogel (or bijel)[25] that solvents are the mixture of oil and water can encapsulate a wider range of active compounds including hydrophilic and lipophilic molecules and will provide more potential applications.[26] Typically, gels are predominantly liquid in composition— 1% to 5% by weight is the gelator and the remaining 95% to 99% is the solvent. When the critical gelation concentration (CGC) is lower than 0.1%, the gelator will be defined as a super-gelator.[27]

Recently, supramolecular gels with multiple stimuli-responsive properties have drawn considerable attention. For example, Zhang and

co-workers prepared a supramolecular gel utilizing a charge transfer interaction between cucurbit[8]urils (CB[8]) and guests, and the resultant gels can be tuned by controlling the self-complementary molecules.[28] Host-guest interactions between crown ethers and organic ammonium salts were effectively used to construct supramolecular gels by Huang's group,[12, 14a] and most of these gels exhibited stimuli-responsive characteristics. Meanwhile, self-healing gels are attracting more and more attentions as well recently.[29] Therefore, we have reasons to believe that the combination of self-healing with multiple (more than four) responsiveness would endow supramolecular materials more fascinating potential applications, which have never been reported. Herein, based on the principle of green chemistry, we employed FA, a natural product, to try to obtain supramolecular gel by tuning the solvent environment. The ratio of good and poor solvents has an important influence on the stability and dynamics of supramolecular architectures, such as the degree of aggregation and equilibrium time, which has been proved by experiments and simulations.[30] FA has been extensively studied due to their anti-tumor effect and G-quartet forming property, and FA salts can form tetramers which can further stack into liquid crystals over a wide range of concentrations induced by alkali ions.[31] Thus, in this work, we utilized DMSO as a good solvent and water as a poor solvent. At certain solvent ratios, the mixed solutions become viscous and eventually transform into gels. Although FA was proved to be a gelator in the DMSO/water system recently,[31j] the detailed mechanism, stimuli-responsiveness, orthogonal self-assemblies as well as self-healing properties have never been explored. With the increase of concentration, topologies of aggregates distinctly change: orthogonal self-assemblies like vesicles, fiber/vesicles, fiber/nanoparticles, nanoparticles could be detected. Induced by the L-gutamic acid moiety of FA, 1-D fibers in gel exhibited helical structures. The orthogonal self-assemblies in this system may provide insights into the mechanisms of differentiation in multi-component cell cultures. Ascribed to the special structure of FA, stimuli including heat, stress, acid, base and light had profound effects on the micro-/macroscopic characteristics of the supramolecular networks. The FA-based supramolecular gel also exhibited a rapid strength recovery according to the magnitude of applied stress. It should be noted that, the DMSO/water solvent environment is also offering more spaces for encapsulating both lipophilic and hydrophilic molecules, which will definitely crest the material.

Experimental section

Materials

All the other reagents are of AR grade and purchased from Country Medicine Reagent Co. Ltd., Shanghai, China. Distilled water was used and DMSO was dried by molecular sieve before used.

Preparing samples for characterization

The FA solution was obtained by adding certain amount of FA into the dried DMSO and stirred to a transparent solution. Then, certain amounts of distilled water were added into a test tube to obtain gels. Light irradiation experiment was performed under xenon lamp (whole range of wavelength, including UV and visible light) for 1 hr and an obvious colour change and phase transition were detected.

Characterization

The samples for TEM were prepared by the phosphotungstic acid staining technique and measured on a JEM-100CX II electron microscope (100 kV). Field-emission scanning electronic microscopy (SEM, Hitachi S-4800) was used to study the microstructure of the hydrogel. Before SEM observation, all the samples were dried in vacuum desiccators for 12h to remove the solvent. AFM images were recorded under ambient condition by using a Veeco Nanoscope Multimode III SPM, and operated in tapping contact mode. The average diameter of vesicles was recorded by DLS measurement with a Wyatt QELS Technology DAWN HELEOS instrument, which used a 12-angle replaced detector in scintillation vial and a 50 mW solid-state laser. The hydrogel was directly tested by a Thermo Scientific HAAKE RheoStress 6000. A DSC 822e thermal analysis system from Mettler-Toledo (Swiss) was employed. The samples (about 3 mg) were weighed into unsealed aluminum pans. The DSC thermogram was recorded with the temperature ranging from 25 to 800 °C at the heating rate of 2 °C/min under a N_2 atmosphere with the reference of empty aluminum. Then the obtained xerogel was mounted onto a copper disk with a double-sided carbon tape and sprayed with gold on the surface. FT-IR measurements were observed by an Avatar370 FT-IR Spectrometer. KBr was used in the process of sample disks preparation. The FT-IR measurements were carried out at room temperature. UV−vis spectra were recorded at room temperature with a TU-1800pc UV−vis spectrophotometer. Circular Dichroism (CD) spectra were measured at room temperature with a JASCO-J810 Circular Dichroism Spectrometer. Mass spectrum (MS) was performed on an Agilent Q-TOF6510 mass spectrometer.

Results and discussion

Phase behaviour

FA (Fig. 1a) has a poor solubility in water while DMSO can well dissolve it. Thus, we chose DMSO and water as good/poor solvents respectively to construct gels. FA solution in DMSO was prepared first and then the distilled water was injected in. At the certain range of concentration and solvent ratio, the mixed solutions became viscous, indicating the formation of aggregates with high molar weight.[32] When the viscous solutions were deposited for a short time, transparent gels were obtained. Fig. 1b shows the different phases with an increase of water content—three phases including solutions, gels and precipitates. It can be observed that the system colors were darker with the ascending of water content, implying the existence of larger aggregates. Interestingly, tiny particles were observed in the gel of 4/6 (DMSO/water, v/v) after being aged for one week and optical microscope proved that they were FA crystals with diameters about 50-

100μm. Crystallization in supramolecular gel phase could provide powerful tools in screening of polymorph of a wide range of organic compounds including pharmaceutical molecules.[33] This phenomenon proved that crystalline growth of the organic compound was facilely achieved in this supramolecular network.

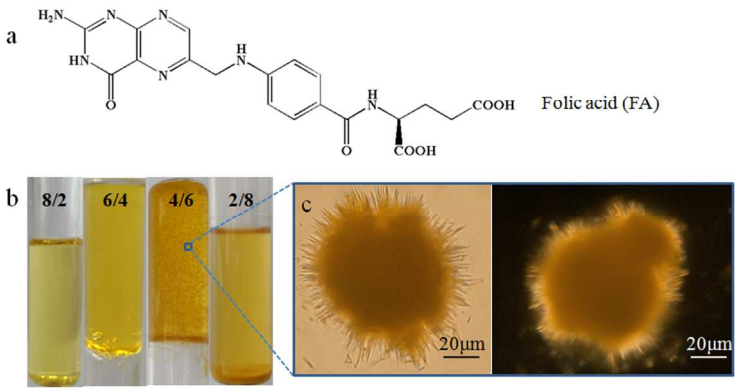

Fig. 1 Structure of FA (a), digital images of FA in different solvent ratios (DMSO/water, v/v, C_{FA}=10 mM) (b), optical microscope images of the aged 4/6 sample under natural and polarized light (c).

Then the detailed phase diagram was plotted and shown in Fig. 2, from which it could be seen that only a certain portion of DMSO or water favoured the gel formation. Other parts formed solutions or precipitates. It can be observed that FA serves as a super-gelator in this system due to the critical gel concentration (CGC) is lower than 0.1 wt%, implying its excellent gelation capability. Besides, the gels have fine optical properties: gels are absolutely transparent, representing the relatively small-size of aggregates. Therefore, the gels can be used as optical devices potentially.[29c] The samples were prepared in the DMSO/water solvent environment which enabled the encapsulation of both lipophilic and hydrophilic molecules. We chose two hydrophilic (RhB, Orange G) and one lipophilic (1-Amino-anthraquinone) dyes as model molecules, which are shown in Fig. S1, ESI. The gels encapsulate these dyes without phase-separations, indicating that this system can serve as a promosing matrix for releasing active compounds. Although these dyes may interact with FA molecules in a non-covalently manner, most of the dyes are existing between the gel networks due to their fine-solubilities in DMSO/water solvents and strong capillarity of porous nanopockets. This speculation can also be verified by the good stability of dye-containing gels and the preservation of micro-morphologies.

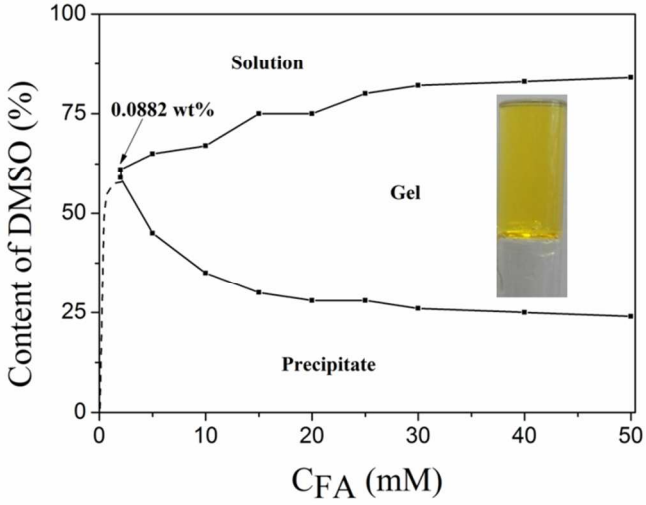

Fig. 2 Phase diagram of FA in DMSO/water system. Dash line: speculated boundary of precipitates and solutions.

Self-assembly of FA and structural analysis

UV-vis spectra and circular dichroism (CD) of FA in mixed solutions were measured and shown in Fig. 3. In the UV-vis spectra (Fig. 3a), the absorbtion peaks of the pterin group appear at 280 and 355 nm. The absorption at 280 nm does not show an noticeable trend with the addition of poor solvents or the increase of concentration. However, the bathocharomically shift from 355 nm to 365 nm indicates that

FA molecules stack in the mixed solvents, resulting from the π-π interactions between pterin rings in a J-type mode.[4c, 34] It can also be found that only gel phases have the red-shift phenomenon and there are no aggregates in DMSO solutions. J-type aggregates, unlike face-to-face H-type, are twisted, which implys the formation of helical structures. This speculation can also be supported by the intensity decrease of peak at 280 nm. To further confirm the hypothesis, CD spectra were performed (Fig. 3b). The CD spectra of 5 mM and 10mM of FA-DMSO solution are inactive and only weak signals were detected owing to the inherent molecular chirality of FA, indicating that there have no aggregates with super-chirality. In contrast, the addition of water gives rise to an active CD signal in the whole absorption wavelength ranges of the pterin ring. Accompanied by the ascending of concentration, cotton effects become more significant. Considering the results of the positive CD spectra, we could envision the formation of ordered chiral structures. As we can see, FA molecule has the molecular chirality, which could further induce the helical stacked arrays.[35] CD results reveal that the molecular chirality is transferred to the central core-pterin ring, and is subsequently amplified in the formation of J-type helical aggregates.

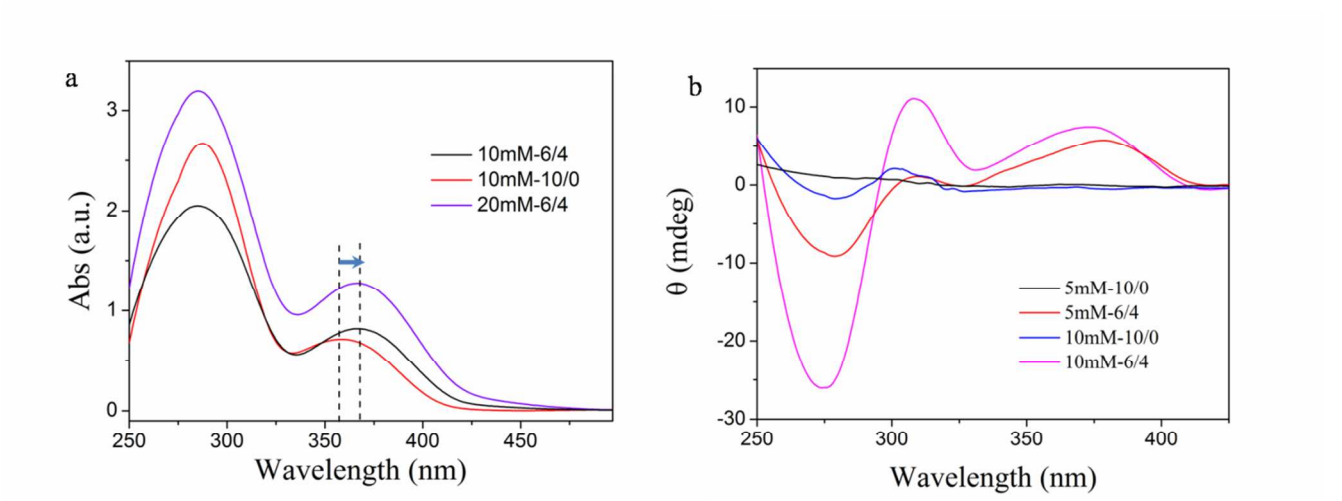

Fig. 3 UV-vis. Spectra (a) and CD spectra (b) of samples with different concentrations and solvent ratios.

The morphologies of samples with different concentrations were probed by TEM and SEM measurements, as shown in Fig. 4 and 5. When the concentration is lower than CGC (2 mM), vesicles with diameters ca. 100~200 nm were detected (Fig. 4a). The presence of vesicles was also detected by the DLS measurement (Fig. 4c). 0.5 mM (DMSO/water, 6/4, v/v) is a critical aggregation concentration, where vesicles and irregular particles are co-existing. Beyond that concentration, such as 1.0 mM, vesicles are the dominant aggregates in solutions. This transition is well elucidated by the change of hydrodynamic radiuses in Fig. 4c. After the gel formation (beyond 2 mM), quite thin fibers with diameters less than 100 nm as well as the vesicles can be observed (Fig. 4d). When the concentration reaches ca. 15 mM, vesicles disappear and solid nanoparticles with diameters lower than 1 μm start to emerge. Meanwhile, fibers start to become thicker which are also probed by the cross section of AFM images (Fig. S2). Solid particles are inlaid in the entangled networks. In the gel of 30 mM, fibers or vesicles totally vanish; only circular solid particles exist and they link to each other to give the free-standing gels. In order to further verify these morphologies, SEM was employed. The results are in accordance with the TEM observations. From Fig. 5b-1, it can be observed that vesicles are embedded in the networks. Sample of 10 mM exhibits thicker fibers and the typical SEM images of vesicles can also be founded in Fig. 5c. Dried hollow spheres with holes and split shells confirm the formation of vesicles. Similar to TEM results, with the increasing of FA concentration, vesicles vanish, while the solid particles appear. Notably, the density of networks is significantly diminished and transformed into solid particles at a high concentration of 30 mM. The surface and size of solid particles and vesicles are entirely different and can be distinguished clearly. As confirmed by UV-vis and CD measurements, twisted 1-D fibers were detected, as shown in the amplified images in Fig. 5f and the inset of d-1. It should be noted that the individual fiber is rather thin: about 10 nm in width. We also estimated the thickness of the nodes in the twisted fibers, which are approximately 4-5 nm. The thickness of the node indicates the basic units of self-assembled structures, and the length of individual FA molecule is about 2 nm. Thus, the thickness of the nodes is in accordance with the length of two FA molecules. Based on the TEM observations, a phase diagram was drawn and shown in Fig. 6. With the increase of concentration, irregular particles, vesicles, nanofiber/vesicles, nanofiber/solid particles and solid particles are the dominant topologies in FA/DMSO/water system. This hierarchical and orthogonal self-assembly will enrich the self-assembly behaviour of natural products.

Cite this: DOI: 10.1039/c0xx00000x

www.rsc.org/xxxxxx

ARTICLE TYPE

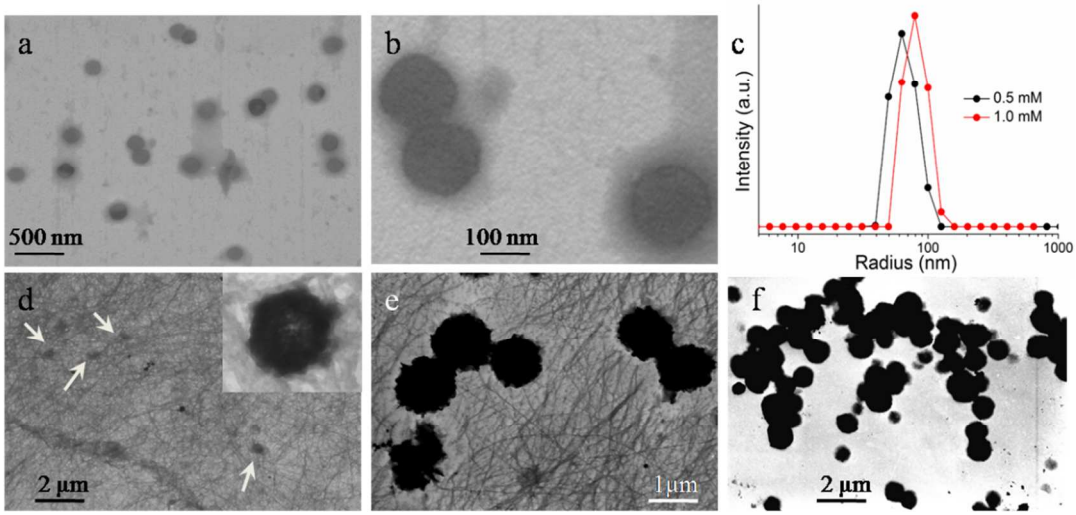

Fig. 4 TEM images of samples with different concentrations, (a-b) 1 mM, (c) DLS distributions of samples with different concentrations, (d) 10 mM (insets: enlarged pictures of vesicles in d), (e) 20 mM, (f) 30 mM.

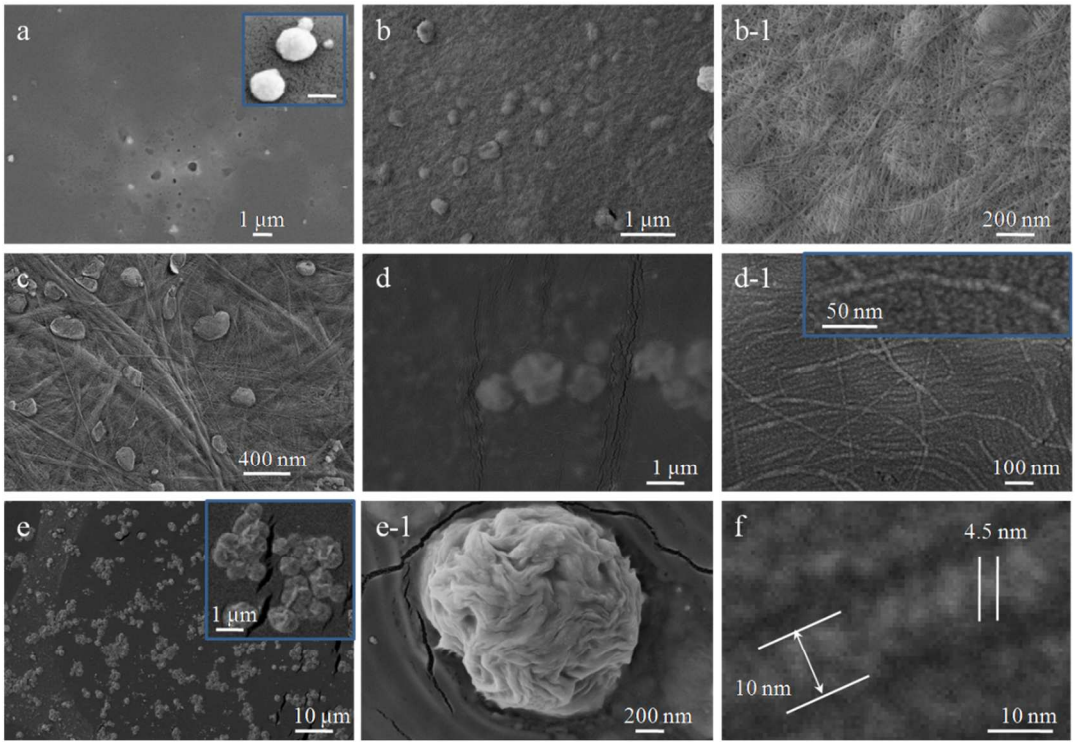

Fig. 5 SEM images, a to e: samples of concentration at 1mM, 5mM, 10mM, 20mM, 30mM (v/v, 6/4) and b-1, d-1 e-1: enlarged images of b, d and e respectively, f: amplified images from images of 5mM; insets: magnified images of vesicles (scale bar: 100 nm), twisted fibers and nanoparticles.

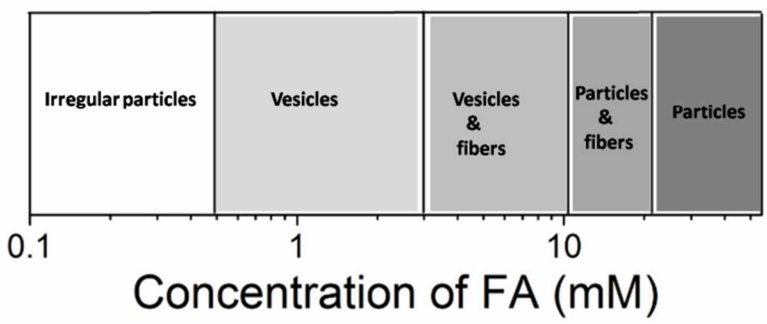

Fig. 6 Phase diagram of the topologies with the concentration of FA on the basis of TEM observations (DMSO/water, 6/4, v/v).

In order to further investigate the mechanism of the morphological evolution, FT-IR (Fig. 7) which can provide insights into the formation of H-bonds was employed. Apart from the π-π stacking interaction, other driving forces for the formation of fibers may be the H-bonds among the pterin rings and the carboxylic acid/amide units. The peak at 1731 cm^{-1} which only emerges in dried gels is due to the *C=O* stretching vibration of H-bonded carboxylic acid groups, indicating the formation of intermolecular H-bonds among carboxylic acid units.[35d] Vibration peaks at 1610, 1540 and 1338 cm^{-1} are assigned to amide-I, amide-II and amide-III bands, respectively. The appearance of these three peaks in dried gels indicates the formation of amide-amide H-bonds. In contrary, only peaks of amide-I, III can be found in native FA spectra. Two peaks at 1510 and 1405 cm^{-1} represent the antisymmetric and symmetric stretching vibrations of carboxylate, and their appearance in gels indicates the destruction of carboxylic acid of FA.[35d-f] The transformation of carboxylic acid to carboxylate may be aroused from proton transfer effect and hydrolyzation in DMSO/water system. Nevertheless, the intensities of peak at 1694 cm^{-1} which is assigned to the carbonyl stretching show no obvious decrease, indicating that only part of the carboxylic acid undergoes proton transfer process.

The pterin ring of folic acid can form two complementary H-bonded arrays: disk-like and ribbon-like.[36] Disk-type always formed through tetramerization of FA and the tetramers have a trend to stack together to give columns which may be the precursors of 1-D twisted fibers.[37] By the way, the width of disk is in consistent with the width of the nodes in amplified SEM images. Ribbon-like arrays has a FA bilayer supported by H-bonds,[38] which fits well with vesicles' membranes. Therefore, the H-bonds of the two arrays may trigger the formation of vesicles and twisted fibers. FT-IR spectra clearly show the same results. Compared with FA, peaks of the amino group/hydroxyl group exhibit a distinct low wavenumber shift which indicates the formation of intermolecular H-bonds (black arrows, Fig. 7b). Combined with these peaks (black arrows), peaks at 3012 cm^{-1} are attributed to the disk-like array and 3150 cm^{-1} ascribed to the ribbon-like pattern.[39] Except for the native FA, other samples have peaks at 3012 cm^{-1}, showing that all gel samples have disk-like H-bonded structures. Peak at 3150 cm^{-1} represents the ribbon-like H-bonded pattern and only emerges in samples at low concentration which also form vesicles.[34] The results further confirm that the disk-like H-bonds contribute to the fiber formation and ribbon-like H-bonds support the vesicle formation.

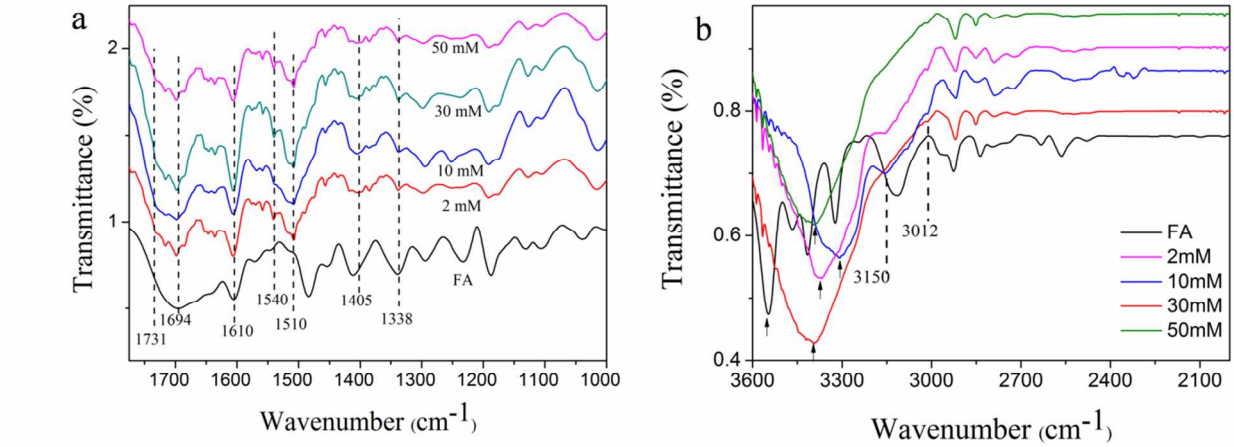

Fig. 7 FT-IR spectra of dried samples with different concentration (v/v 4/6).

According to the results, a schematic model of the structural evolution in self-assembly process was drawn and showed in Fig. 8. On the basis of the experimental results, the size of aggregates increases significantly with the increase of FA concentration from 1 mM to 50 mM (from vesicles, fibers to nanoparticles). According to the equation[41]:

$$\mu_N = \mu_\infty + \frac{\alpha kT}{N_p} \quad (1)$$

the decrease of the aggregation number (N) is proportional to the increase of the mean interaction free energy per molecule (μ_N) which is compensated by the elimination of the unfavorable rim energy of the fibers by its closing up into smaller size aggregates such as vesicles (*vice versa*). This equation indicates that, with the increase of concentration, the discrete 1-D fibers stack together into thicker fibers and the thicker fibers will grow up into solid particles thermodynamically. It should be noted that, because of the micro-phase separation structures or orthogonal self-assemblies in the supramolecular system, a decreased net number of elastically effective crosslinks will be given. The net-loss of the total number of crosslinks may contribute remarkably weaker net-strength than the strength of isolated supramolecular crosslinks. As a consequence, both the dynamics and mechanical strength might be affected, which would be discussed in the next part.

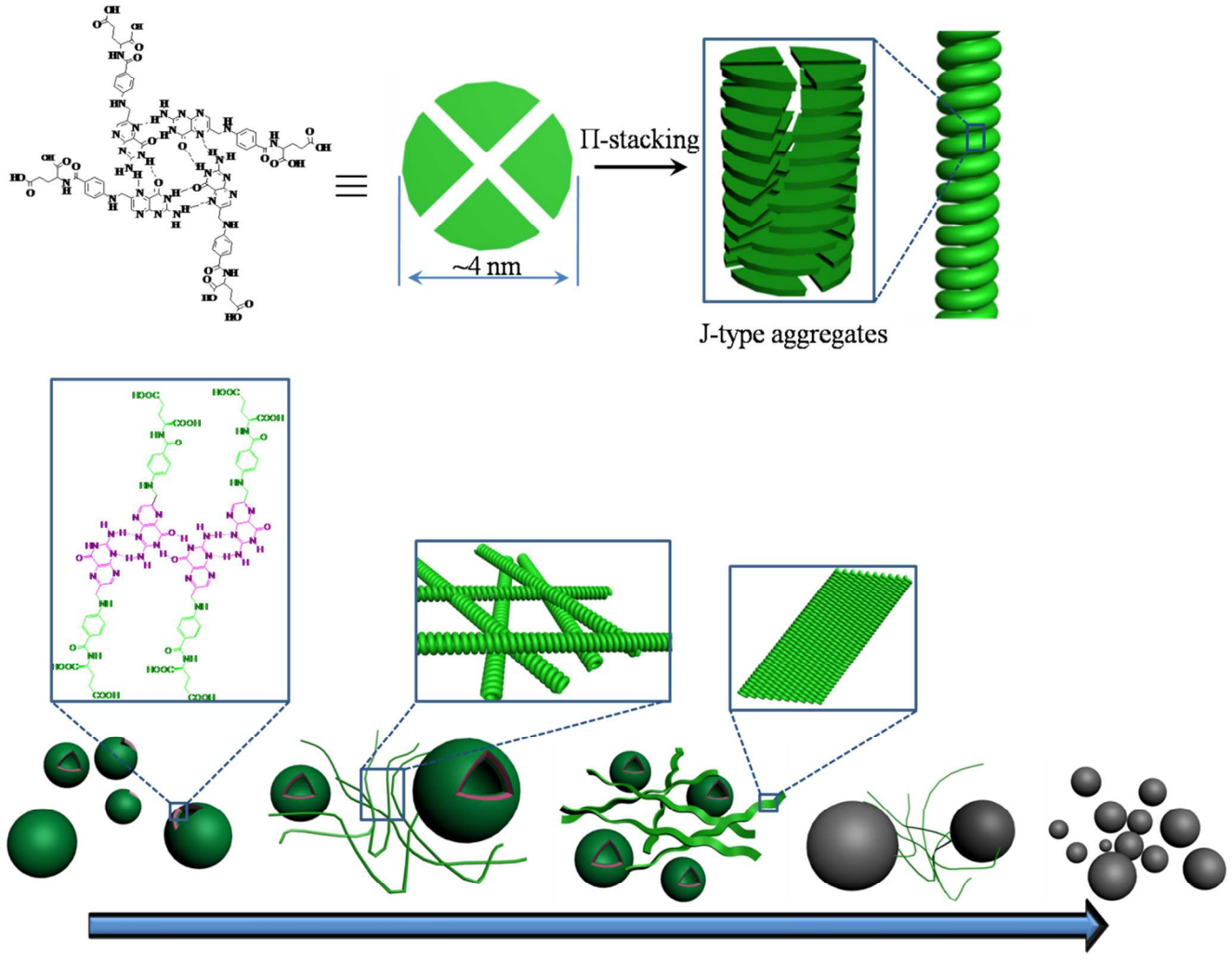

Fig. 8 Schematic representation of the formation mechanism of the topological evolution with the increase of concentration.

Rheological studies

Rheological studies of different supramolecular networks were investigated to address the diversity of mechanical properties. Dynamic oscillatory stress sweep and frequency sweep are shown in Fig. 9. The strain response to an applied stress can be depicted by two dynamic modulus which are the elastic modulus (G′: solid-like behaviour) and viscous modulus (G″: liquid-like behaviour). The solid nature of all samples can be characterized by the fact that, in the linear viscoelastic region, the storage moduli (G′) are higher than the loss-moduli (G″). Beyond the linear viscosity region, G′ falls behind G″ and the gel transforms into a liquid-like appearance. Thus, under high oscillatory stress, the solid-like gel begins to flow. The name "yield stress" is the value of the crossover of G″ and G′, representing the stiffness.[42] From the concentration and solvent ratio-dependent stress sweeps (Fig. 9a), we can conclude that, the stiffness is in a positive correlation with the concentration of FA or poor solvent content (water). Frequency sweep indicates that, G′ values of all

performed samples are much higher than that of G″ over the entire range of frequency range. Both the G′ and G″ of samples show the frequency-independent behaviour (Fig. 9b), indicating the existence of the weak matrix in the gel.[43] Results of frequency sweep provide the values of G′, which reflects the mechanical strength. The concentration-dependent sweep shows that the mechanical strength is ascending with the increase of concentration, due to more and longer fibers entangle together. Gel networks will be strengthened when more water participates in the self-assembly process (Fig. 9c and d). Through the analysis of the rheologies, the mechanical properties such as mechanical stress and yield stress can be tailored facilely through controlling the composition (concentration, good/poor solvents) of the gels. The concentration-dependent behaviour of mechanical strength is ascribed to the fact that the aggregation degree may be related to association constant Ka and the concentration.[16] Thus, mechanical properties are controlled by concentration because Ka is only related to temperatures. As well, contents of poor solvents have a profound effect on the nucleation and elongation (degree of aggregation or polymerization) as well as the entanglement of the nano-fibers.

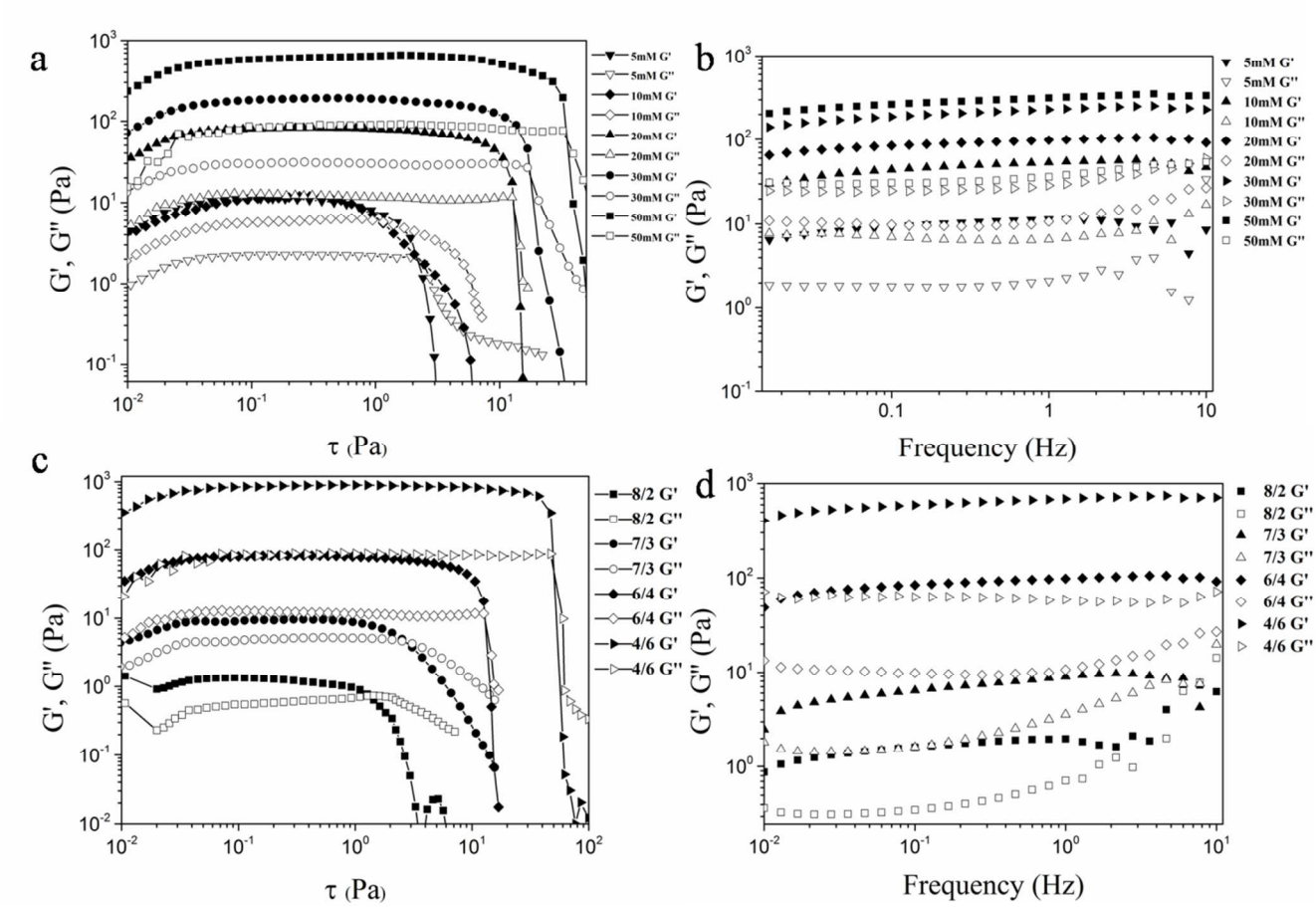

Fig. 9 Dynamic oscillatory stress sweep and frequency sweep of samples with different concentrations (6/4, v/v) and different solvent ratios (concentration fixed at 20mM), respectively.

Dynamics

Complex plateau modulus G_N of gels can be given by the following equation (2). For a self-assembled gel network, the number of entanglement sites related to an average molar weight between effective crosslinks (Me) at short times can be predicted by equation (3), where ρ is the concentration of the solution (g/m^3), R is the molar gas constant, and T is the absolute temperature.[44] For supramolecular gels or supramolecular polymeric gels, there might be deriving scaling laws for system parameters like G_N and viscosity as functions of gelator concentrations.[45-47] For FA/DMSO/water system, these functions were deduced and shown in Fig. 10.

$$G_N = \sqrt{G'^2 + G''^2} \qquad (2)$$

$$G_N = \frac{\rho RT}{Me} \qquad (3)$$

G_N values are plotted as the functions of concentration in Fig. 10a on a double-logarithmic scale. For the whole range of concentration (C), a relationship $G_N \propto C^{1.5}$ was obtained. Therefore, the elasticity in FA/mixed solvent system is a consequence of the entangled effect between long, flexible supramolecular linear fibers formed in this system.[47] At the region of high concentration, nanoparticles are dominant structures in the system, which may affect the relationship of G_N and concentration. Using Eq. 3, the average molar weights

between effective crosslinks were calculated from plateau moduli G_N and shown in Fig. 10b. Larger values for Me represent the less number of effective crosslinks. It can be observed that, with the increase of concentration or water content, Me diminishes sharply, indicating the formation of more crosslinks.[46] More crosslinks in systems give rise to the enhanced mechanical stress and contracted structures, and the trends of concentration- or water content-dependent Me are in accordance with the rheological studies and morphological evolutions. According to the linear viscoelasticity, the zero-shear viscosity η_0 can be determined precisely in the lower frequency region. Fig. 10c exhibits the concentration dependence of η_0 on a double-logarithmic scale. We could see that, η_0 shows a linear behaviour, and the slopes at lower and high concentration scales show discrepant values that demonstrate the solution/gel boundary obviously. In the gel phase, a slope value of 1.45 was obtained, indicating a relationship of $\eta_0 \propto C^{1.45}$. The exponent 1.45 is smaller than value predicted by the supramolecular polymeric gel model. This behaviour may be derived from the orthogonal self-assemblies where a portion of FA participates in the formation of vesicles. Losing of the effective crosslink numbers gives rise to a negative effect on the dynamic viscosities of supramolecular systems.

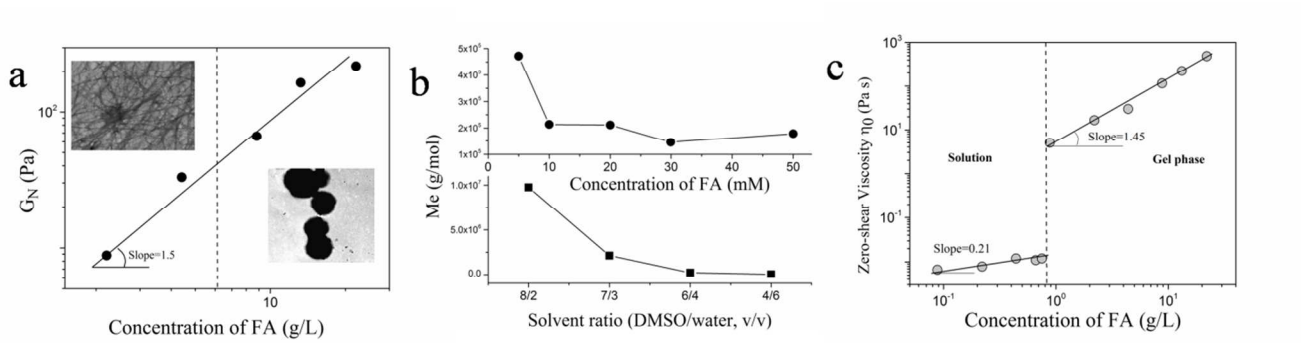

Fig. 10 Complex modulus (G_N) as a function of concentration, a, insets: dominant structures at low and high concentration; average molecular weights between effective cross-Links (Me) of various concentrations and solvent ratios, b; relationship between zero-shear viscosity and concentrations, c. Solvent ratios of all samples for concentration-dependent test are fixed at 6/4.

Self-healing behaviour and its application

As a fascinating characteristic of material, self-healing often occurs in supramolecular system.[9] As well as the elastomer,[48] networks of gels show this feature.[29, 49] Chemical gels recover very slowly after being broken down by shear due to the low mobility of large macromolecules.[50] Generally, self-healing should include two parts: shape-recovery and strength recovery,[51] while only strength recovery will be discussed here. FA-mixed solvent system exhibits a rapid strength recovery after being broken down. As shown in the left image of Fig. 11, stress amplitude sweeps of the sample demonstrate an elastic response of gels. Under larger amplitude oscillatory force (stress = 40 Pa, f = 1 Hz), G′ falls from 500 Pa to 0.5 Pa and G″ is higher than G′, resulting in a liquid phase. When the amplitude returns (stress = 0.5 Pa, f = 1 Hz), the gel recovers its 90% strength to be a solid state. This process can be repeated at least 5 times without irreversible weakening. The rapid recovery of mechanical strength can be attributed to the physical nature of supramolecular networks and the relatively low molecular mass of building blocks. The gel's responsiveness to shear forces is useful for several applications. For example, inks in ink-jet printers should be the liquid state when be squirted out the pen, but a solid state is needed when they touch the paper. As shown in the right image of Fig. 11, the work "Gel" was written by an injector on a coverslip. In the needle of the injector, gels are runny upon pressing, while they could hardly flow when touching the slip. This property reveals that the supramolecular gels are mouldable and applicable.

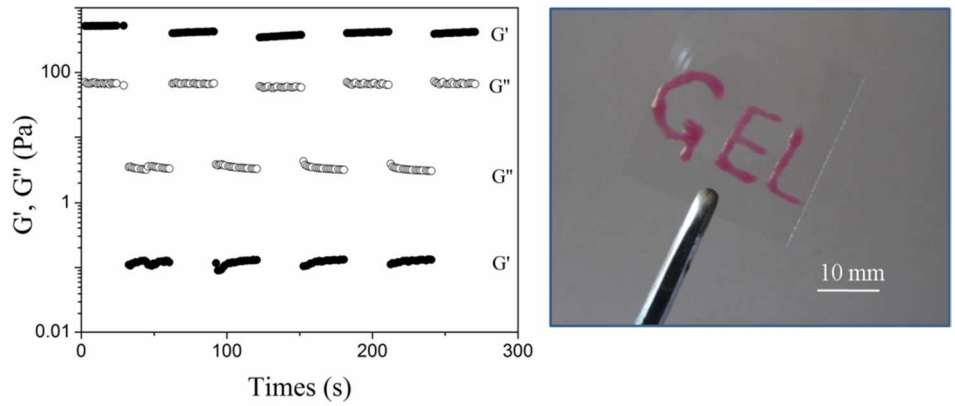

Fig. 11 Left-image: G′ and G″ values of gel (50 mM, 6/4) in continuous stress measurements. The sample was subject to 40 Pa for 30 s, then back to 0.5 Pa in the linear regime for 30 s, and this process was repeated for 5 times. The scanning frequency was 1 Hz. Right image: RhB carried gel as inks and the written character on a coverslip.

Thermal Responsiveness

Temperature which determines the binding constant strongly influences the extension/crosslinking of the linear supramolecular nanofibers in gels. Therefore, supramolecular gel networks are quite sensitive to temperature, particularly near the critical gelling temperature. As shown in Fig. 12, concentration and solvent ratio dependent DSC curves show the endothermic peaks from 40 to 80 ^{o}C, which account for the gel-solution phase transitions. We noticed that, with the increase of concentration on the same solvent ratio, transition temperatures exhibited an increasing trend, whereas the absorbed heat or the change of enthalpy was not affected. In contrary, solvent ratio-dependent DSC results show a conflict trend: the enthalpy changes with the increase of water content. Variations in temperature will bring about changes of chain reptation and breaking, which are relating to the activation energy E_a. In supramolecular gel system, $E_a = (E_{a,\,rep} + E_{a,\,break})/2$; the activation energy E_a is contributed by the reptation and breaking of the chains, and thus the chain breaking cannot be not affected by concentration.[46] These results are well-demonstrated by the activation energy theory as elucidated above.

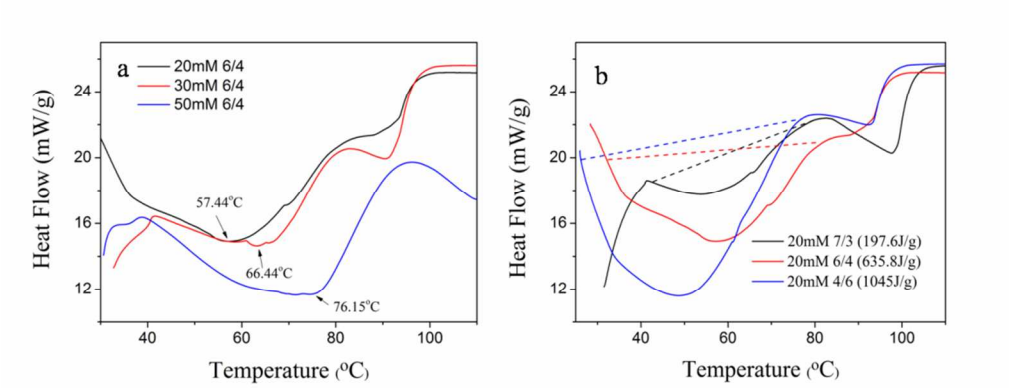

Fig. 12 DSC curves of samples with different concentrations and solvent ratios.

Effects of other poor solvents

Apart from water, other poor solvents particularly alcohols could also be used to fabricate supramolecular gel networks, as demonstrated in Fig. 13. We found that water had the most exceptional capability to build up robust networks although glycerine given the similar mechanical strength due to its high viscosity. The mechanical strength should relate to the hydroxyl values. When lowering the hydroxyl values, both the yield stress and G′ of the samples show a steep decrease. This result implied that, the mechanical properties can be tuned by changing poor solvents.

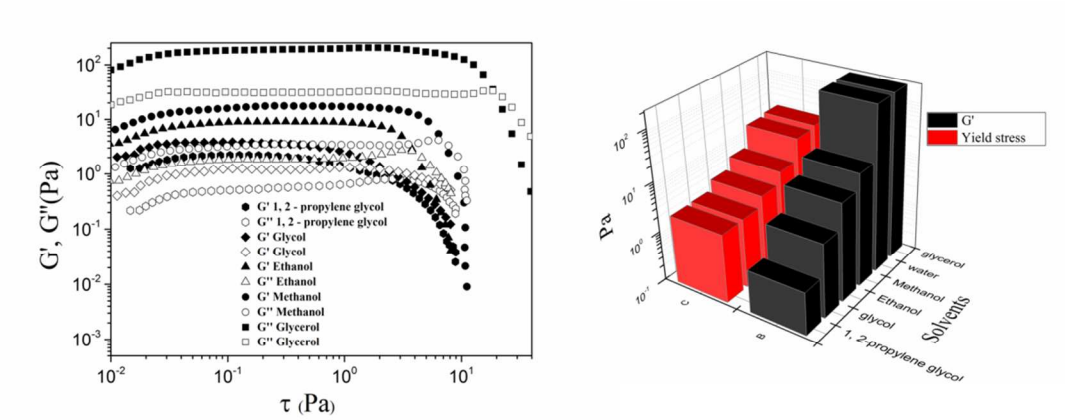

Fig. 13 Results of G′ (linear region) and yield stress of samples fabricated by other poor solvents and DMSO (v/v 4/6, 30mM).

Multiple Responsiveness

From the above results, we have known that the formation of 1-D supramolecular nanofibers in this system is supported by H-bonds and π-π stacking. If these interactions are disturbed, the properties of gels will be changed. As demonstrated in Fig. 14, the amino atoms of pterin moiety are easily affected by protonation, which would denature the original H-bonds. Light particular UV light can cleavage FA into pterin and aminobenzoyl glutamate[52], and base would turn FA into a water soluble compound or disturb the intermolecular carboxylic H-bonds (proton transfer). It is proposed that, in spite of applied stress and heat, factors including acid, light and base can be utilized as stimuli to tune the self-assemblies of FAs. It should be noted that, stimuli like acid, base and light could arouse permanent structure change of FA, and resulted in the irreversible responsive properties.

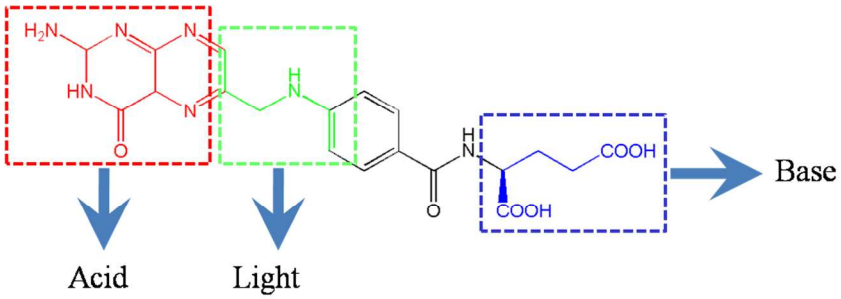

Fig. 14 Molecular formula of FA and its sensitive groups which can be affected by the three stimuli.

As expected, by adding acid (concentrated HCl solution) or base (here is solid NaOH) directly onto the gel surface, a rapid gel-to-solution phase transition was observed (Fig. 15a-b). Tyndall effect (F.g. 15c) reveals that the addition of base/acid disassociates the self-assembled structures. In order to investigate their effects, acid or base was permixed in water before preparing gels. As shown in Fig. 15d and e, for a 10 mM gel sample, only a small amount of NaOH would turn gels into solutions. Notably, at certain range of NaOH concentrations, weak gels formed and then transformed into viscous solutions after being deposited for one week. It implies that the networks are quite sensitive to base. However, the addition of acid would strengthen the gels in a wide concentration region; transparent gels become turbid after adding HCl, indicating the formation of aggregates with larger size. Meanwhile, the G′ values are extremely elevated: from 10 Pa to ca. 1000 Pa. This enhancement of two orders of magnitude may be derived from the increase of crosslinks or the appearance of thicker fibers. When 2 eq. HCl was added, the modulus reaches the maximum value: 6000 Pa. Nevertheless, when more acid was mixed, the modulus falls sharply: 3 eq. of HCl only gives a solution.

For the sake of the detailed mechanism of the acid/base-responsiveness, UV-vis and CD were employed, as shown in Fig. S3. The two peaks at 280 and 360 nm change obviously. Peaks at 360 nm diminish with the increase of acidity and disappear finally with the addition of 3 eq. HCl (Fig. S3a). Meanwhile, the absorbance peak at 280 nm is increased after acidification. These variations are due to the disassembly of stacked tetramers.[53] The CD spectra (Fig. S3c) confirm the disassemble process; both the negative and positive cotton effects become inactive and the intensities of the CD signals decrease significantly. When NaOH was mixed in the system, UV-vis (Fig. S3b) spectra changed as well. Addition of 0.2 eq. or fewer bases would trigger the disassembly of π stacked tetramers as indicated by the blue shifts at 360 nm, which is also verified by CD spectra (Fig. S3d). When more than 2 eq. NaOH was added, larger red shifts reformed. It is assumed that the abundant addition of metal ions (Na^+) favours the formation of π stacked aggregates. However, the details still need further investigation.

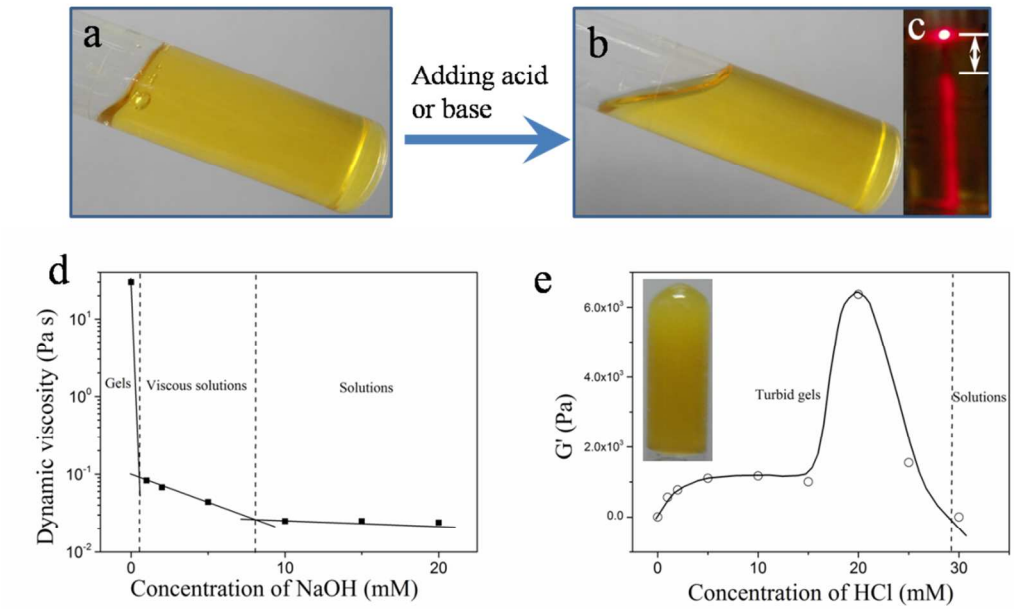

Fig. 15 Images of the phase transition by adding acid or base (a, b); tyndall effect in the process of gel-solution transition (c); dynamic viscosity of samples (10mM, 6/4, f = 0.1 Hz, applied stress = 0.5 Pa) with the concentration variations of premixed NaOH (d); G′ of samples (10mM, 6/4, f = 1 Hz, applied stress = 0.5 Pa) with the concentration variations of premixed HCl (e), inset: image of turbid gel.

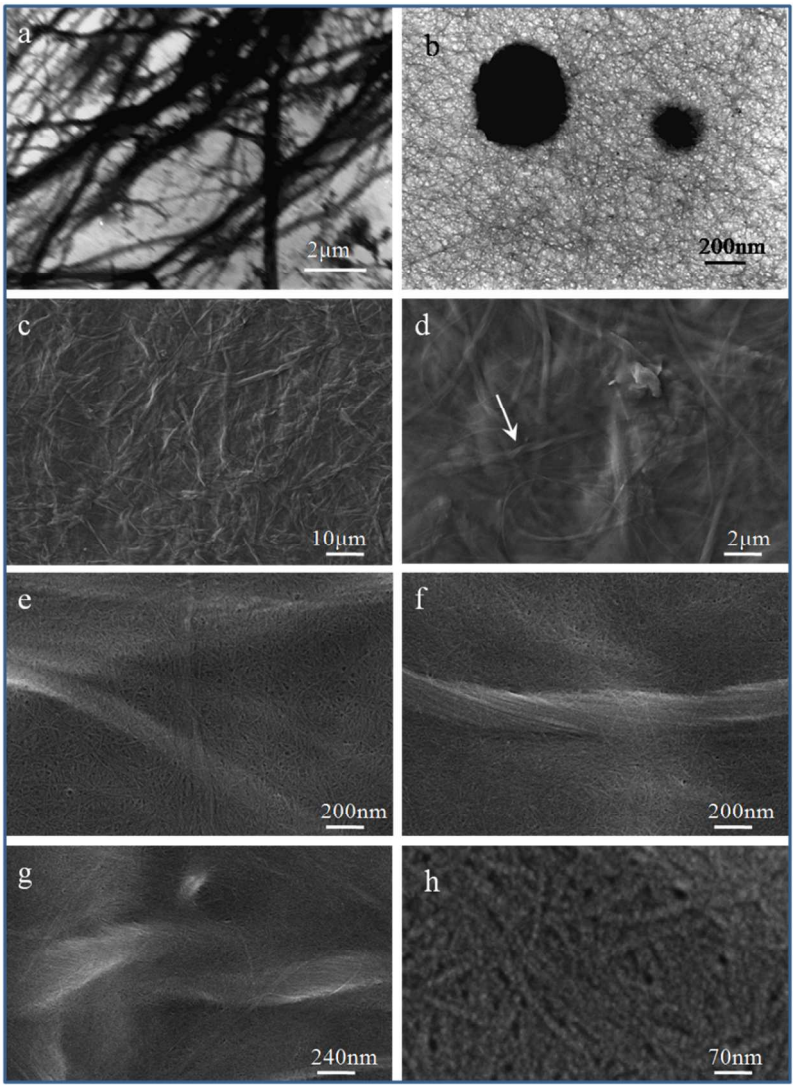

Fig. 16 TEM images of samples with 20mM HCl (a) and 2 mM NaOH (b); SEM images of 20 mM HCl samples with different magnifications (c-h). Concentrations of all samples are fixed at 10 mM and ratio at 6/4 (DMSO/water, v/v).

Gel's responsiveness to acid and base were further explored by the microscope. As elucidated above, samples without base or acid have very thin fibers which are hardly detected by an optical microscope. However, the addition of HCl turns transparent gels into turbid gels that micro-morphologies can be clearly observed by the optical microscope (Fig. S4, ESI). Fibers become thicker after adding acid: up to hundreds of nanometres. Addition of 2 eq. HCl which gives the strongest gel (Fig. 15e) has the extremely thicker fibers (more than 1 μm in width). These results are in good consistent with the rheological studies. Then, TEM and SEM images (Fig. 16) confirm the morphologies of the optical microscope results. In contrast to HCl, samples containing NaOH exhibit a similar morphology to the previous gels (Fig. 16b). It is proposed that base affects the solubility of FA and disturb the H-bonds between carboxylic acids in water, diminishing the number of 1-D fibers. SEM images with different magnifications reveal the hierarchical self-assemblies after adding HCl. We could observe that larger aggregates were composed of very thin fibers. These thin fibers pack together to give larger fibers and these thicker fibers also show a slightly helical structure (arrow in Fig. 16d) which is in agreement with optical microscopic studies (Fig. S4f). Acid definitely results in the formation of the secondary-assembled structures. Apart from the appearance of large structures, the extensive existence of thin fibers is detected as well. Although the CD spectra imply the decreased cotton effect upon the addition of HCl, thin helical and twisted fibers were also found (Fig. 16h). Acid may enhance the intermolecular H-bonds of FA tetramers, which induces the secondary assembly of individual fibers to form larger fibers.

As described in Fig. 7, there would be a proton transfer effect for FA molecules in DMSO/water system, which may contribute greatly to the duplex responsiveness to acid and base. Carboxylic acid moieties play a vital role in the self-aggregation behaviour of FA. The protonation or deprotonation can strengthen and weaken the driving forces of self-assembly respectively. In or before the self-assembly process, protons from part of carboxylic acids would transfer to the amine groups, and this effect hinders the self-aggregation of these FA

molecules because the intermolecular H-bonds are not favored. As a consequence, only small amount of base could turn gels into the solutions. However, in a slight acidic environment, some carboxylates are protonated, resulting in the strengthened aggregation, and thicker fibers/robust gels will form. Definitely, an excess amount of acids will protonate all the amino groups and turn the gels into solutions.

Due to the light sensitive property of FA, light was introduced as a stimulus to trigger the structural change of self-assembled FA. Remarkably, fiber-containing gels transformed into dark colored precipitates (inset of Fig. S5) upon light irradiation with a whole range of wavelength for 1hr. We detected that acidity environment would accelerate the photolysis process. UV-vis spectra imply that the concentration of FA in the matrix was diminished remarkably after light irradiation, due to the decrease of the relative absorbance at 280 and 360 nm. Meanwhile, the absorbance at the wavelength of visible region (around 600 nm) is elevated. These changes indicated the structural changes of FA. Then the precipitates as well as the solution were dispersed in DMSO and performed on the MS measurement (Fig. S6). Peak at 442 attributed to $FA{\cdot}H^+$ occupies a small portion, representing that a large portion of FA have been degraded. At the same time, new peaks emerge: peaks at 179 and 267 which represent the pterin and aminobenzoyl glutamate fragment, respectively. Supramolecular gels have been photo-degraded successfully and this characteristic could be used to achieve the smart release applications .

Conclusions

In conclusion, we have demonstrated the fabrication of multiple responsive supramolecular gel with a self-healing property through the good/poor solvent strategy. The building block FA behaves as a super-gelator that can form gel in DMSO/water, which provides a matrix for encapsulating both lipophilic and hydrophilic molecules. Orthogonal self-assemblies and structural evolution including vesicles, fiber/vesicles, fiber/nanoparticles, nanoparticles are achieved in this system. It should be noted that the molecular chiral glutamate moiety induces the supramolecular helical structures of the 1-D fibers. The self-healing property enables this gel to be applicable in ink or painting areas. Multi-responsiveness to heat, acid, base, as well as light were investigated and offered facile ways to fabricate smart materials. As the first example of multi-responsive supramolecular gel stem from native FA through solvent strategy, this system as well as the method provides an efficient and "green" path for fabricating functional supramolecular materials.

Notes and references

[a]*School of Chemistry and Chemical Engineering and Key Laboratory of Colloid and Interface Chemistry of Ministry of Education, Shandong University, Jinan 250100, PR China. Fax: +86 531 88564464; Tel: +86 531 88363306; E-mail: haoay@sdu.edu.cn.*

† Electronic Supplementary Information (ESI) available: [details of any supplementary information available should be included here]. See DOI: 10.1039/b000000x/

1 (a) K. Wang, D. Guo, X. Wang and Y. Liu, *ACS Nano*, 2011, **5**, 2880; (b) D. Guo, K. Wang, Y. Wang and Y. Liu, *J. Am. Chem. Soc.*, 2012, **134**, 10244; (c) Q. Duan, Y. Cao, Y. Li, X. Hu, T. Xiao, C. Lin, Y. Pan and L. Wang, *J. Am. Chem. Soc*., 2013, **135**, 10542; (d) P. Xing, T. Sun, A. Hao, *RSC Adv*., 2013, **3**, 24776.

2 (a) L. Li, M. Rosenthal, H. Zhang, J. J. Hernandez, M. Drechsler, K. H. Phan, S. Rtten, X. Zhu, D. A. Ivanov, and M. Mçller, *Angew. Chem. Int. Ed*., 2012, **51**, 11616; (b) T. T. Larsen, A. Bjarklev, D. S. Hermann, and J. Broeng, *Opt. Express*, 2003, **11**, 2589; (c) P. Blake, P. D. Brimicombe, R. R. Nair, T. J. Booth, D. Jiang, F. Schedin, L. A. Ponomarenko, S. V. Morozov, H. F. Gleeson, E. W. Hill, A. K. Geim and K. S. Novoselov, *Nano Lett.*, 2008, **8**, 1704; (d) T. Kato, N. Mizoshita, and K. Kishimoto, *Angew. Chem. Int. Ed*., 2006, **45**, 38.

3 (a) A. M. Kloxin, M. W. Tibbitt & K. S. Anseth, *Nat. Protoc*., 2010, **5**, 1867; (b) Cole A. DeForest and Kristi S. Anseth, *Nat. Chem.*, 2011, **3**, 925; (c) N. Park, S. H. Um, H. Funabashi, J. Xu and D. Luo, *Nat. Mater*., 2009, **8**, 432.

4 (a) T. Aida, E. W. Meijer, S. I. Stupp, *Science*, 2012, **335**, 813; (b) L. Brunsveld, B. J. B. Folmer, E. W. Meijer, and R. P. Sijbesma, *Chem. Rev*., 2001, **101**, 4071; (c) T. F. A. De Greef, M. M. J. Smulders, M. Wolffs, A. P. H. J. Schenning, R. P. Sijbesma, and E. W. Meijer, *Chem. Rev*., 2009, **109**, 5687.

5 C. Fouquey, J.-M. Lehn, A. M. Levelut, *Adv. Mater*., 1990, **2**, 254.

6 O. A. scherman, *Nat. Chem*., 2009, **1**, 524.

7 A. W. Bosman, R. P. Sijbesma, and E. W. Meijer, *Mater. Today*, 2004, **1369**, 34.

8 S. Li, T. Xiao, C. Lin and L. Wang, *Chem. Soc. Rev*., 2012, **41**, 5950.

9 T. F. A. de Greef and E. W. Meijer, *Nature*, 2008, **453**, 171.

10 (a) Q. Wang, J. L. Mynar, M. Yoshida, E. Lee, M. Lee, K. Okuro, K. Kinbara and T. Aida, *Nature*, **2010**, *463*, 339; (b) S. Burattini, H. M. Colquhoun, B. W. Greenland and W. Hayes, *Faraday Discuss*., 2009, **143**, 251.

11 J. Li, J. A. Viveros, M. H. Wrue and M. Anthamatten, *Adv. Mater*., 2007, **19**, 2851.

12 X. Yan, F. Wang, B. Zheng and F. Huang, *Chem. Soc. Rev*., 2012, **41**, 6042.

13 (a) L. Fang, M. Hmadeh, J. Wu, M. A. Olson, J. M. Spruell, A. Trabolsi, Y. Yang, M. Elhabiri, A. Albrecht-Gary, and J. F. Stoddart, *J. Am. Chem. Soc*., 2009, **131**, 7126; (b) G. Du, E. Moulin, N. Jouault, Eric Buhler, and N. Giuseppone, *Angew. Chem. Int. Ed*., 2012, **51**, 12504; (c) L. Zhao, K. Wang, L. Xu, Y. Liu, S. Zhang, Z. Li, Y. Yan and J. Huang, *Soft Matter*, 2012, **8**, 9079; (d) L. Jiang, Y. Yan and J. Huang, *Soft Matter*, 2011, **7**, 10417.

14 (a) B. Zheng, F. Wang, S. Dong and F. Huang, *Chem. Soc. Rev*., 2012, **41**, 1621; (b) S. Dong, B. Zheng, D. Xu, X. Yan, M. Zhang, and F. Huang, *Adv. Mater*., 2012, **24**, 3191.

15 (a) S. Burattini, B. W. Greenland, D. Chappell, H. M. Colquhoun and W. Hayes, *Chem. Soc. Rev*., 2010, **39**, 1973; (b) Y. Lin, Y. Qiao, P. Tang, Z. Li and J. Huang, *Soft Matter*, 2011, **7**, 2062. (c) Y. Lin, X. Cheng, Y. Qiao, C. Yu, Z. Li, Y. Yan and J. Huang, *Soft Matter*, 2010, **6**, 902.

16 S. Seiffert and J. Sprakel, *Chem. Soc. Rev*., 2012, **41**, 909.

17 A. Noro, M. Hayashi and Y. Matsushita, *Soft Matter*, 2012, **8**, 6416.

18 (a) P. Terech, R. G. Weiss, *Chem. Rev.*, 1997, **97**, 3133; (b) N. M. Sangeetha, U. Maitra, *Chem. Soc. Rev.*, 2005, **34**, 821; (c) M. M. Piepenbrock, G. O. Lioyd, N. Clarke, J. W. Steed, *Chem. Rev*., 2010, **110**, 1960.

19 L. E. Buerkle and S. J. Rowan, *Chem. Soc. Rev*., 2012, **41**, 6089.

20 (a) J. W. Steed, *Chem. Commun*., 2011, **47**, 1379; (b) J. G. Hardy, A. R. Hirst, D. K. Smith, C. Brennan and I. Ashworth, *Chem. Commun*., 2005, 385; (c) R. K. Das, R. Kandanelli, J. Linnanto, K. Bose and U. Maitra, *Langmuir*, 2010, **26**, 16141.

21 A. Brizard, M. Stuart, K. van Bommel, A. Friggeri, M. de Jong and J. van Esch, *Angew. Chem. Int. Ed*., 2008, **47**, 2063.
22 T. Kato, *Science*, 2002, **295**, 2414.
23 A. Heeres, C. van der Pol, M. Stuart, A. Friggeri, B. L. Feringa and J. H. van Esch, *J. Am. Chem. Soc*., 2003, **125**, 14252.
24 J. Nanda, A. Biswas, B. Adhikari, and A. Banerjee, *Angew. Chem. Int. Ed*., 2013, **125**, 5045.
25 M. E. Cates, and P. S. Clegg, *Soft Matter*, 2008, **4**, 2132.
26 M. E. Helgeson, S. E. Moran, H. Z. An and P. S. Doyle, *Nat. Mater.*, 2012, **11**, 344.
27 (a) S. Dong, B. Zheng, D. Xu, X. Yan, M. Zhang, and F. Huang, *Adv. Mater*., 2012, **24**, 3191; (b) M. Žini, F. Vögtle , F. Fages, *Top. Curr. Chem.*, 2005, **25**, 39; (c) D. Yu, X. Huang, M. Deng, Y. Lin, L. Jiang, J. Huang and Y. Wang, *J. Phys. Chem. B*, 2010, **114**, 11725.
28 Y. Liu, Y. Yu, J. Gao, Z. Wang, and X. Zhang, *Angew. Chem*., 2010, **122**, 6726.
29 (a) M. Zhang, D. Xu, X. Yan, J. Chen, S. Dong, B. Zheng, and F. Huang, *Angew. Chem. Int. Ed*., 2012, **51**, 7011; (b) P. C. Franc ¸O Tournilhac, C. S. Ziakovic & L. Leibler, *Nature*, 2008, **451**, 977; (c) A. Vidyasagar, K. Handore, and K. M. Sureshan, *Angew. Chem. Int. Ed*., 2011, **50**, 8021; (d) N. R. Sottos & J. S. Moore, *Nature*, 2011, **472**, 299; (e) M. Nakahata, Y. Takashima, H. Yamaguchi & A. Harada, *Nat. Commun*., 2011, **2**, 511.
30 (a) P. A. Korevaar, C. Schaefer, T. F. A. de Greef, and E. W. Meijer, *J. Am. Chem. Soc*., 2012, **134**, 13482; (b) W. Weng, Z. Li, A. M. Jamieson, and S. J. Rowan, *Macromolecules*, 2009, 42, 236.
31 (a) P. Xing, X. Chu, G. Du, M. Li, J. Su, A. Hao, Y. Hou, S. Li, M. Ma, L. Wu and Q. Yu, *RSC Adv*., 2013, **3**, 15237; (b) R. H. Fung Cheung, J. G. Hughes, P. J. Marriott and D. M. Small, *Food Chem.*, 2009, **112**, 507; S. Salmaso, A. Semenzato, and P. Caliceti, *Bioconjugate Chem.*, 2004, **15**, 997; (c) P. Garin-Chesa, I. Campbell, P. E.Saigo, J. L. Jr. Lewis, L. J. Old, and W. Rettig, *J. Am. J. Pathol.*, 1993, **142**, 557; (d) H. Wang, C. Yang, L. Wang, D. Kong, Y. Zhang and Z. Yang, *Chem. Commun.,* 2011, **47**, 4439; (e) L. Perez-Alvarez, V. Saez-Martinez, E. Hernaez, M. Herrero, I. Katime, *Macromol. Chem. Phys*., 2009, **210**, 467; (f) S. Nayak, H. Lee, J. Chmielewski, and L. A. Lyon, *J. Am. Chem. Soc*., 2004, **126**, 10258; (g) T. Kato, T. Matsuoka, M. Nishii, Y. Kamikawa, K. Kanie, T. Nishimura, E. Yashima, and S. Ujiie, *Angew. Chem. Int. Ed.*., 2004, **43**, 1969; (h) N. Sakai, Y. Kamikawa, M. Nishii, T. Matsuoka, T. Kato, and S. Matile, *J. Am. Chem. Soc*., 2006, **128**, 2218; (i) J. T. Davis, *Angew. Chem. Int. Ed*., 2004, **43**, 668; J. T. Davis and G. P. Spada, *Chem. Soc. Rev.*, 2007, **36**, 296; (i) M. Ceborska, M. Zimnicka, M. Pietrzak, A. Troć, M. Koźbiał and J. Lipkowski, *Org. Biomol. Chem.*, 2012, **10**, 5186; (J) P. Chakraborty, B. Roy, P. Bairi and A. K. Nandi, *J. Mater. Chem*., 2012, **22**, 20291.
32 (a) T. Haino, A. Watanabe, T. Hirao, and T. Ikeda, *Angew. Chem. Int. Ed*., 2012, **51**, 1473; (b) S. Dong, Y. Luo, X. Yan, B. Zheng, X. Ding, Y. Yu, Z. Ma, Q. Zhao, and F. Huang, *Angew. Chem. Int. Ed*., 2011, **50**, 1905.
33 (a) A. R. Hirst, B. Escuder, J. F. Miravet, and D. K. Smith, *Angew. Chem. Int. Ed*., 2008, **47**, 8002; (b) J. A. Foster, M. M. Piepenbrock, G. O. Lloyd, N. Clarke, J. A. K. Howard and J. W. Steed, *Nat. Chem*., 2010, **2**, 1037.
34 (a) C. Chen, and T. Ong, *J. Am. Chem. Soc.*, 2013, **135**, 5294; (b) E. E. Jelley, *Nature*, 1936, **138**, 1009.
35 (a) C. Zhan, P. Gao, M. Liu, *Chem. Commun*., 2005, 462; (b) X. Wang, P. Duan, M. Liu, *Chem. Commun*., 2012, **48**, 7501; (c) P. Duan, X, Zhu, M. Liu, *Chem. Commun.*, 2011, **47**, 5569. (d) C. Zhan, P. Gao and M. Liu, *Chem. Commun*., 2005, 462–464. (e) P. Gao, C. Zhan and M. Liu, *Langmuir,* 2006, **22**, 775; (f) Q. Jin, L. Zhang and M. Liu, *Chem. Eur. J*., 2013, **19**, 9234.
36 K. Kanie, T. Yasuda, S. Ujiie, T. Kato, *Chem. Commun*., 2000, 1899.
37 (a) F. Ciuchi, G. D. Nicola, H. Franz, G. Gottarelli, P. Marisni, M. G. P. Bassi, and G. P. Spada, *J. Am. Chem. Soc*., 1994, **116**, 7064; (b) N. Sakai, Y. Kamikawa, M. Nishii, T. Matsuoka, T. Kato, and S. Matile, *J. Am. Chem. Soc*., 2006, **128**, 2218.
38 (a) Takashi Kato, *Science*, 2002, 295, 2414; (b) L. Zhang, K. Yu, A. Eisenberg, *Science*, 1996, **272**, 1777.
39 K. Kanie, M. Nishii, T. Yasuda, T. Taki, S. Ujiie and T. Kato, *J. Mater. Chem*., 2001, **11**, 2875.
40 T. Kato, T. Matsuoka, M. Nishii, Y. Kamikawa, K. Kanie, T. Nishimura, E. Yashima, and S. Ujiie, *Angew. Chem. Int. Ed*., 2004, **43**, 1969.
41 M. Wang, A. R. Mohebbi, Y. Sun, and F. Wudl, *Angew. Chem. Int. Ed*., 2012, **51**, 6920. In this equation, μ_N is the standard part of the chemical potential or the mean interaction free energy per molecule in aggregates of aggregation number N; μ_∞ is the total energy of a molecule in an infinite aggregate; α is a positive constant; T is absolute temperature (K); k is Boltzmann constant; p is a number that depends on the shape or dimensionality of the aggregates.
42 J. W. Steed, *Chem. Soc. Rev*., 2010, **39**, 3686.
43 H. Wang, C. Yang, L. Wang, D. Kong, Y. Zhang and Z. Yang, *Chem. Commun*., 2011, **47**, 4439.
44 J. W. Goodwin, R. W. Hughes, Rheology for Chemists, an Introduction; The Royal Society of Chemistry: Cambridge, 2000.
45 M. E. Cates, *Macromolecules*, 1987, **20**, 2289.
46 T. Vermonden, M. J. van Steenbergen, N. A. M. Besseling, A. T. M. Marcelis, W. E. Hennink, E. J. R. Sudholter, and M. A. Cohen Stuart, *J. Am. Chem. Soc*., 2004, **126**, 15802.
47 A. Ciferri, Supramolecular Polymers, Taylor & Francis Group, 2nd edn, 2005.
48 Y. Chen, A. M. Kushner, G. A. Williams and Z. Guan, *Nat. Chem.*, 2012, **4**, 467.
49 (a) E. A. Appel, X. J. Loh, S. T. Jones, F. Biedermann, C. A. Dreiss and O. A. Scherman, *J. Am. Chem. Soc*., 2012, **134**, 11767; (b) K. Imato, M. Nishihara, T. Kanehara, Y. Amamoto, A. Takahara, and H. Otsuka, *Angew. Chem. Int. Ed*., 2012, **51**, 1138; (c) T. Kakuta, Y. Takashima, M. Nakahata, M. Otsubo, H.Yamaguchi, and A. Harada, *Adv. Mater*., 2013, DOI: 10.1002/adma.201205321.
50 A. P. Nowak, V. Breedveld, L. Pakstis, B. Ozbas, D. J. Pine, D. Pochan and T. J. Deming, *Nature*, 2002, **417**, 424.
51 (a) C. Wang, W. Huang, Z. Ding, Y. Zhao, H. Purnawali, L. Zheng, H. Fan and C. He, *Smart Materials and Structures*, 2012, **21**, 115010; (b) J. Zhang, W. Huang, H. Lu, L. Sun, *Materials and Design*, 2014, **53**, 1077.
52 E. L. Wittle, B. L. O'Dell, J. M. Vandenbelt and J. J. Pfiffner, *J. Am. Chem. Soc*., 1947, **69**, 1786.
53 Y. Kamikawa, M. Nishii, and T. Kato, *Chem. Eur. J*., 2004, **10**, 5942.

